Environmental Science & Technology

Article

pubs.acs.org/est

Selective Aptamers for Detection of Estradiol and Ethynylestradiol in Natural Waters

Spurti U. Akki,[†] Charles J. Werth,*[,†,‡] and Scott K. Silverman*[,§]

[†]Department of Civil and Environmental Engineering, University of Illinois at Urbana−Champaign, 205 North Mathews Avenue, Urbana, Illinois 61801, United States

[‡]Department of Civil, Architectural and Environmental Engineering, University of Texas at Austin, 301 East Dean Keeton Street, Austin, Texas 78712, United States

[§]Department of Chemistry, University of Illinois at Urbana−Champaign, 600 South Mathews Avenue, Urbana, Illinois 61801, United States

Supporting Information

ABSTRACT: We used in vitro selection to identify new DNA aptamers for two endocrine-disrupting compounds often found in treated and natural waters, 17β-estradiol (E2) and 17α-ethynylestradiol (EE). We used equilibrium filtration to determine aptamer sensitivity/selectivity and dimethyl sulfate (DMS) probing to explore aptamer binding sites. The new E2 aptamers are at least 74-fold more sensitive for E2 than is a previously reported DNA aptamer, with dissociation constants (K_d values) of 0.6 μM. Similarly, the EE aptamers are highly sensitive for EE, with K_d of 0.5−1.0 μM. Selectivity values indicate that the E2 aptamers bind E2 and a structural analogue, estrone (E1), equally well and are up to 74-fold selective over EE. One EE aptamer is 53-fold more selective for EE over E2 or E1, but the other binds EE, E2, and E1 with similar affinity. The new aptamers do not lose sensitivity or selectivity in natural water from a local lake, despite the presence of natural organic matter (~4 mg/L TOC). DMS probing suggests that E2 binding occurs in relatively flexible single-stranded DNA regions, an important finding for rational redesign of aptamers and their incorporation into sensing platforms. This is the first report of aptamers with strong selectivity for E2 and E1 over EE, or with strong selectivity for EE over E2 and E1. Such selectivity is important for achieving the goal of creating practically useful DNA-based sensors that can distinguish structurally similar estrogenic compounds in natural waters.

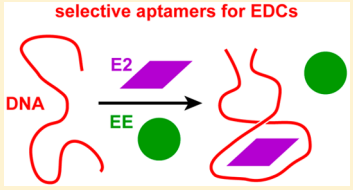

INTRODUCTION

Endocrine-disrupting compounds (EDCs) compose a class of emerging contaminants that are a growing concern due to their negative impacts on human and aquatic life.[1−6] They originate from various municipal, industrial, and institutional sources including wastewater effluent and solid waste, as well as from feedlot runoff containing animal waste. Among the EDCs, 17β-estradiol (E2), 17α-ethynylestradiol (EE), and estrone (E1) (Figure 1A) have been widely detected in groundwater and surface water samples (~nM).[7] The EPA included these three compounds in the list of contaminants that require monitoring in public water samples from 2013 to 2015 in accordance with the Unregulated Contaminant Monitoring Rule 3 (UCMR3). Of these contaminants, E2 and EE have the highest estrogenic potencies.[8,9] Therefore, sensitive, selective, rapid, and inexpensive methods for detection of E2 and EE in natural water samples are needed.

The current state-of-the-art for EDC detection includes chromatographic−spectroscopic methods (e.g., LC-MS, GC-MS) and antibody-based molecular recognition assays such as ELISAs (enzyme-linked immunosorbent assays). The former techniques are associated with high sensitivity (~pM)[10,11] but are expensive, sometimes require extensive sample pretreatment (e.g., sample derivatization), are instrumentation- and time-intensive, and cannot be practically used for real-time analysis. The antibody-based molecular recognition assays are sensitive enough for natural samples (~nM to pM)[12,13] and are relatively inexpensive, but they can suffer from poor selectivity due to interference by analogues and matrix components.[14−16] Additionally, antibodies used in ELISAs need to be harvested from animals, which makes the process time-consuming[17] and a social concern.[18]

An emerging field in sensor studies is based on molecular recognition by single-stranded DNA or RNA oligonucleotides called aptamers. Especially for DNA, the low-cost synthesis of an aptamer, coupled with its tolerance to a wide range of physiological conditions compared to antibodies, suggests that aptamers can be used in complex environmental matrixes. Moreover, aptamers can be readily functionalized to facilitate their integration into a variety of sensor platforms. Aptamer-based sensors,[19−28] also called aptasensors, can have high sensitivity (as low as fM)[29−31] and can be employed for real-time detection of contaminants and other compounds.[32−34]

To date, only a single aptamer for E2 or its analogues has been reported. It does not discriminate strongly among E2, E1, and EE, and a binding constant as low as 0.13 μM was reported by Kim et al.[35] This published aptamer (no particular

Received: May 14, 2015
Revised: July 14, 2015
Accepted: July 16, 2015
Published: July 16, 2015

DOI: 10.1021/acs.est.5b02401
Environ. Sci. Technol. 2015, 49, 9905−9913

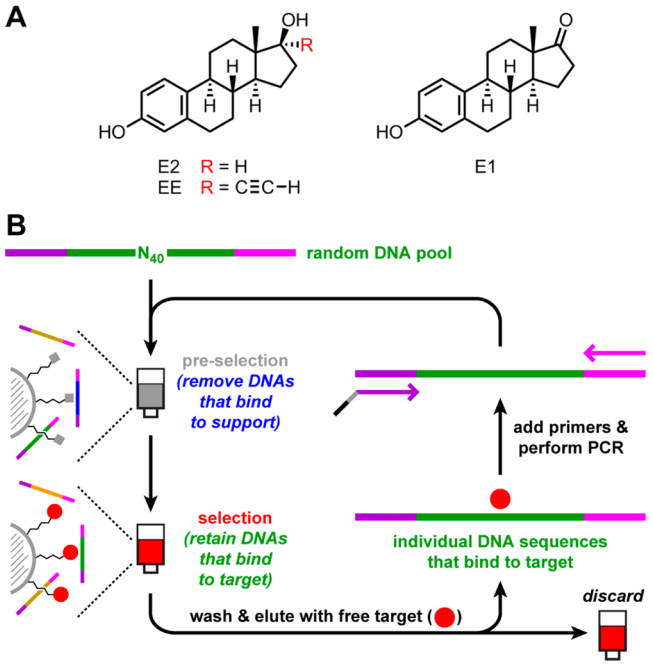

Figure 1. 17β-Estradiol (E2) and its derivatives, 17α-ethynylestradiol (EE) and estrone (E1), and in vitro selection strategy for identification of aptamers. (A) E2, EE, and E1. (B) In vitro selection strategy.

designation was used in ref 35) has been integrated into a number of sensing platforms, with detection based on fluorescence,[36] a color change,[37] or an electrochemical signal.[35,38] Sensors developed using this aptamer had detection limits for E2 as low as 33 fM[30] and good binding affinity in natural waters.[27,30] These reports highlight the improved detection limits of aptamer-based sensors relative to the binding affinities of the aptamers themselves. While these reports represent a major step forward in real-time monitoring of E2 in natural waters, greater selectivity for E2 over its analogues is needed to create sensors for selective monitoring of the many different estrogenic compounds of varying concentrations in natural waters.

The objectives of this study are to use in vitro selection to identify a new suite of DNA aptamers that bind with high sensitivity and selectively to E2 or EE; to determine if binding affinities change in natural waters that contain nontarget constituents (e.g., natural organic matter); and to explore the binding regions of the selected aptamers. We used in vitro selection, often called SELEX (Systematic Evolution of Ligands by EXponential enrichment),[39,40] to identify DNA aptamers for E2 and EE (Figure 1B). Selection pressures were applied by increasing elution times to elute stronger binding aptamers (which have lower off-rates) or by decreasing eluent concentrations to identify aptamers that are sensitive to lower concentrations of the target. The equilibrium filtration assay was used to determine DNA binding affinities to E2, E1, and EE in clean selection buffer as well as in both tap water and natural water from a small urban lake, each amended with selection buffer after a one-step filtration. Binding affinities were used to determine sensitivities of the DNA aptamers, while the ratio of sensitivities for one EDC to another was used to calculate selectivities of the aptamers. Dimethyl sulfate (DMS) probing was used to methylate guanosine nucleotides of aptamers in the presence of the target compound (E2 or EE), with the expectation that only guanosine nucleotides not involved in the binding interaction with the target compound are accessible for methylation. Insights from these results suggest potential approaches for rational improvement of DNA aptamers.

EXPERIMENTAL SECTION

Materials. The EDCs E2 (>98%), E1 (>99%), and EE (>98%) were obtained from Sigma-Aldrich. Tritiated EDCs 2,4,6,7-^{3}H-E2 (81 Ci/mmol) and 2,4,6,7-^{3}H-E1 (94 Ci/mmol) were purchased from PerkinElmer, and 6,7-^{3}H-EE (60 Ci/mmol) was obtained from American Radiolabeled Chemicals. DMS (dimethyl sulfate, >99%) was obtained from Acros. DNA oligonucleotides were prepared by solid-phase synthesis on an ABI 394 instrument using reagents from Glen Research or purchased from Integrated DNA Technologies (IDT). The oligonucleotides were purified either by PAGE (polyacrylamide gel electrophoresis) or phenol/chloroform extraction, followed by ethanol precipitation. For PAGE purification, 7 M urea denaturing PAGE was used with running buffer TBE (89 mM each Tris and boric acid, 2 mM EDTA, pH 8.3), and oligonucleotides were extracted from the polyacrylamide with TEN buffer (10 mM Tris, pH 8.0, 1 mM EDTA, 300 mM NaCl). DNA oligonucleotides used in selections contained 40 consecutive random nucleotides (N_{40}) with known primer-binding regions on both ends (see Supporting Information (SI) for details).

Immobilization of E2 and EE on Agarose Support. E2 and EE were immobilized on epoxy-activated agarose support (Sepharose 6B, GE Healthcare, catalog number 17-0480-01) by reaction of the phenolic hydroxy group of E2/EE with the epoxy group. The extent of derivatization was quantified by UV−visible spectroscopy (see SI for details).

In Vitro Selection Procedure. We performed in vitro selection, seeking E2-selective and EE-selective aptamers. The selection strategy (Figure 1B) involved an initially random N_{40} pool of DNA sequences, of which 0.1% was 5′-^{32}P radiolabeled, in binding buffer (50 mM Tris, pH 7.5, 5 mM $MgCl_2$, and 300 mM NaCl). We chose a 40-nucleotide random region as a trade-off between the ease of incorporating shorter aptamers into sensors and improved sensitivity and selectivity of long aptamers due to more complex folding. This DNA pool was exposed to agarose support contained in a preselection column to eliminate sequences that bind to the support at room temperature (23 °C). The flow-through from the preselection column was exposed to immobilized (agarose support-bound) E2/EE contained in a selection column. The selection column was washed with binding buffer containing 20% ethanol to remove any nonspecifically bound sequences. The E2/EE-bound sequences were eluted for a total of 1 h from the selection column with binding buffer containing 200 μM E2 or binding buffer containing 20 μM EE. Eluted sequences were PCR-amplified and taken into the next selection round (the desired, forward single strand was separable because the reverse strand was initiated with a primer that includes a nonamplifiable spacer). After each round, the binding activity of the pool was quantified according to the fraction of sequences that eluted specifically with E2/EE. For rounds 9+ of the E2 selection, a longer elution time pressure was applied (6 h total elution time) to promote elution of tighter-binding sequences. In the EE selection, a lower eluent concentration of EE was used as a concentration pressure from the beginning of the selection to identify aptamers that were sensitive to lower concentrations of EE. After 10 rounds of both selections, cloning and sequencing

DOI: 10.1021/acs.est.5b02401
Environ. Sci. Technol. 2015, 49, 9905−9913

of the pools were performed. The clones were screened using a preliminary binding assay with immobilized E2/EE (see SI for details).

Determining Aptamer Dissociation Constants (K_d Values) for E2 and Analogues by Equilibrium Filtration Assay. In the equilibrium filtration assay, a known DNA aptamer concentration was incubated in a 1.7 mL tube with 0.5 μM of EDC (including ~5 nM ^{3}H-EDC) in 200 μL of binding buffer with 2% (v/v) ethanol for 1 h at 23 °C. (For assays of the published aptamer from ref 35, their reported buffer was used instead: 100 mM Tris, pH 8.0, 10 mM $MgCl_2$, 200 mM NaCl, 25 mM KCl, and 5% ethanol.) The solution was transferred to a 10000 MW cutoff filter (Microcon YM-10, Millipore) and centrifuged at 5000g for 10 min. The volume of filtrate, v_F, was measured (±2 μL) by pipet; a typical value was 90−95 μL. The filtrate was transferred to a 7 mL HDPE scintillation vial containing 5 mL of scintillation fluid (EcoScint O, National Diagnostics). The inner column of the cutoff filter was inverted and centrifuged at 1000g for 3 min to collect the retentate, for which the volume, v_R, was typically 85−90 μL. The retentate was similarly transferred to a scintillation vial. The inner column was washed with 2 × 300 μL of selection buffer (5 min incubation in inner tube, inversion, and centrifugation). Finally, the inner tube was flushed with 2 × 300 μL of ethanol by centrifugation at 17200g for 15 min. A scintillation counter (Beckman Coulter LS 6500) was used to quantify amounts of ^{3}H. For the retentate, the counts, c_R, were taken as the sum of the counts in the retentate and the two washes. For the filtrate, the counts, c_F, were taken as the sum of the counts in the filtrate and the two flushes.

The chemical binding equilibrium between an aptamer and its ligand is governed by eq 1, where A is the DNA aptamer and L is the ligand (here E2, EE, or E1). The equilibrium constant for this reaction, which is the dissociation constant K_d, is representative of the binding affinity of the aptamer to the ligand. Lower values of K_d indicate better binding affinities of the aptamer with the ligand. The total concentration c of L was fixed at 0.5 μM, although in several cases other values of c (e.g., 10 μM) were evaluated experimentally, with quantitatively similar outcomes (data not shown). The total DNA aptamer concentration, a, was varied from 0.01 to 50 μM. The concentration in a particular sample of the aptamer−ligand (A·L) complex, y, is related to c and a by eq 2. Solving for y leads to eq 3.

$$\underset{y}{\mathrm{A{\cdot}L}} \rightleftharpoons \underset{a-y}{\mathrm{A}} + \underset{c-y}{\mathrm{L}} \tag{1}$$

$$K_d = \frac{(a-y)(c-y)}{y} \tag{2}$$

$$y = \frac{(c+a+K_d) - \sqrt{((c+a+K_d)^2 - 4ca)}}{2} \tag{3}$$

Equation 3 is used to determine K_d, where y is derived from the experimental data using eq 4. The midpoint of the plot of y versus a (as in Figure 2A) is derived from eq 3 by taking $y = c/2$, which results in eq 5. This allows correlation of the visually apparent midpoint with the actual K_d value; there is an offset of $c/2$.

$$y = \left(\frac{C_R - C_F \times \frac{v_R}{v_F}}{C_R + C_F}\right) \times c \tag{4}$$

$$a_{1/2} = K_d + \frac{c}{2} \tag{5}$$

In some cases, the data did not fit the model represented by a simple bimolecular interaction given by eq 1. Similar cases showing more complex DNA aptamer binding have been reported,[31,41] and we applied eq 6, which incorporates a Hill coefficient, n, in order to accommodate the degree of cooperativity in binding. The equilibrium constant K_d for eq 6 is described by eq 7.

$$\underset{y}{\mathrm{A{\cdot}L}_n} \rightleftharpoons \underset{a-y}{\mathrm{A}} + \underset{c-ny}{n\mathrm{L}} \tag{6}$$

$$K_d = \frac{(a-y)(c-ny)^n}{y} \tag{7}$$

As seen from eq 7, the concentration of the complex A·L$_n$, y, cannot be easily separated from the independent variable (a) and fit variables (K_d, n). Therefore, we used MATLAB to cover a landscape of K_d and n values and computed y for a given range of values of a. The best fit values of K_d and n were found by minimizing the root-mean-square error between the computed and experimentally derived values of y. The plots with the Hill coefficient model fits are in the SI (Figure S4), with errors of the fit values computed as described in the SI.

For certain combinations of aptamer and ligand with weak binding, precise K_d values could not be determined because a limiting concentration of the aptamer−ligand complex could not be reached. In such cases, the lower limit of K_d was estimated as the maximum DNA concentration at which the data was obtained, i.e., $K_d \geq 50$ μM.

For ease of comparison of different aptamers, a half-saturation constant $K_{1/2} = K_d^{1/n}$ was calculated, where $K_{1/2}$ represents the concentration of the ligand at which half the aptamer sites are occupied. When an aptamer−ligand interaction was modeled well by eq 1, $n = 1$ and $K_{1/2} = K_d$. Selectivity of the each aptamer for the parent ligand (E2 or EE) over its analogues was evaluated by taking the ratio of the half-saturation constants, i.e., $K_{1/2,\mathrm{analogue}}/K_{1/2,\mathrm{parent}}$.

DMS Probing. Probing by dimethyl sulfate (DMS) was used to interrogate the folded structures of nucleic acids. Each 5′-^{32}P-radiolabeled aptamer was incubated with a series of concentrations of E2 or EE, followed by treatment with DMS, which methylates the physically accessible N7 nitrogen atoms of guanosine nucleotides (see SI for full procedures).[42] Such methylation blocks the enzymatic activity of DNA polymerase, which therefore allows readout of the methylation sites. The DMS accessibilities of individual nucleotides change as the aptamer folds, typically by decreasing because the initially accessible N7 atoms become buried within the folded structure. The samples were treated with piperidine followed by PAGE. The methylated guanine nucleobases are good leaving groups, such that treatment with base (10% piperidine) leads to depurination followed by base-promoted strand scission (Figure 4A). Each PAGE band corresponds to a unique and assignable guanosine nucleotide of the aptamer. Band intensities for guanosine nucleotides that changed with E2/EE concentration were quantified and normalized.

Band intensities for individual guanosine nucleotides were first normalized within each lane to a particular guanosine nucleotide whose intensity did not appear to depend upon E2/EE concentration (G45 for E2Apt1, G56 for E2Apt2, G57 for EEApt1, and G38 for EEApt2). For each nucleotide, the

DOI: 10.1021/acs.est.5b02401
Environ. Sci. Technol. 2015, 49, 9905−9913

resulting band intensities were renormalized to a value of 1 for the band intensity at the lowest nonzero E2/EE concentration of 1 nM. The final normalized band intensity was plotted against the concentration of E2/EE (c) according to eq 8, leading to a K_d value as determined from the data for that nucleotide. Fitted parameters I_{low} and I_{high} are the limiting band intensities at low and high concentrations of EE/EE. All fitted values of I_{low} were 1.00 ± 0.03. The DMS probing data were modeled well by the equilibrium of eq 1, and therefore the more complicated fitting process associated with the equilibrium of eq 6 was unnecessary.

$$I_{obs} = \left(\frac{I_{low} + I_{high} \times \frac{c}{K_d}}{1 + \frac{c}{K_d}} \right) \quad (8)$$

RESULTS

Identification of E2-Selective Aptamers. In vitro selection was performed to identify E2-selective aptamers (Figure 1B). The E2-binding activity was undetectable above background (~3%) until rounds 7 and 8, where 29% and 24% of the pool were bound to the immobilized E2 and then specifically eluted by free E2 with a 1 h elution step (Figure S1). Selection pressure for tighter binding (i.e., lower value of the dissociation constant, K_d) was imposed by increasing the elution time to 6 h, which enables elution of aptamers with slower off-rate and therefore tighter binding. In rounds 9 and 10 with the longer elution time, 23% and 35% binding were observed. Individual E2 aptamers were cloned from round 10 and screened according to their ability to bind to immobilized E2. On this basis, 16 unique E2-binding sequences were identified; these sequences did not segregate into any specific families (not shown). Preliminary experiments were performed, involving both (1) immobilized E2-binding assays analogous to the binding step used during selection itself and (2) dimethyl sulfate (DMS) probing experiments as described below. On the basis of these preliminary data, two aptamers designated as E2Apt1 and E2Apt2 (Figure S2) were studied in greater detail because of their high binding affinities.

Characterization of E2-Selective Aptamers by Equilibrium Filtration Assay. The equilibrium filtration assay was used to quantify binding constants for E2Apt1 and E2Apt2, as well as the E2 aptamer reported by Kim et al.[35] The assays for the published aptamer were performed in the binding buffer reported in ref 35. The equilibrium distribution profile for E2Apt1 is shown in Figure 2A (same for E2Apt2 as shown in Figure S3); the E2 data is not fit well at high E2 concentration by the curve corresponding to eq 3. Therefore, we used the Hill coefficient model of eqs 6 and 7, which allowed a better fit to the entire data set (Figure S4). E2Apt1 and E2Apt2 were found to have K_d values for E2 of 0.60 and 0.56 μM, respectively, with Hill n values for E2 of 1.3 and 1.5, respectively (see Table 1 for tabulation of all K_d and n values in this report). In parallel, we determined a reproducible and unexpectedly high K_d value ≥50 μM (with Hill n = 1) for the E2 aptamer reported by Kim et al.[35] (Figure S3), although its K_d was reported by those authors as 0.13 μM. We cannot explain this discrepancy in K_d for the E2 aptamer from ref 35, but we are confident in the reproducibility of our measurements, which were made with each aptamer not immobilized in any way.

The equilibrium filtration assay was also used to assess K_d of E2Apt1 and E2Apt2 for binding to the E2 analogues E1 and EE. The Hill n values for the analogues were 1, as the data fit well to eq 3. To facilitate comparisons of aptamer sensitivity, we plotted in Figure 2B inverse K_d values of E2Apt1 and E2Apt2 for each of E2, E1, and EE binding, where higher values correspond to better sensitivity. We observe that E2Apt1 and E2Apt2 bind with greatest affinity to E2 followed by E1 and last EE. For each E2 analogue, the aptamer selectivity was quantified as $K_{1/2,analogue}/K_{1/2,E2}$, where $K_{1/2} = K_d^{1/n}$ represents the EDC concentration at which the aptamer is half-saturated. Both aptamers gave similar results for their selectivity (Figure 3). Each aptamer bound to E1 nearly as well as E2, with only 4−7-fold selectivity for E2. In contrast, each aptamer bound much less well to EE than to E2, with ≥74-fold selectivity for E2.

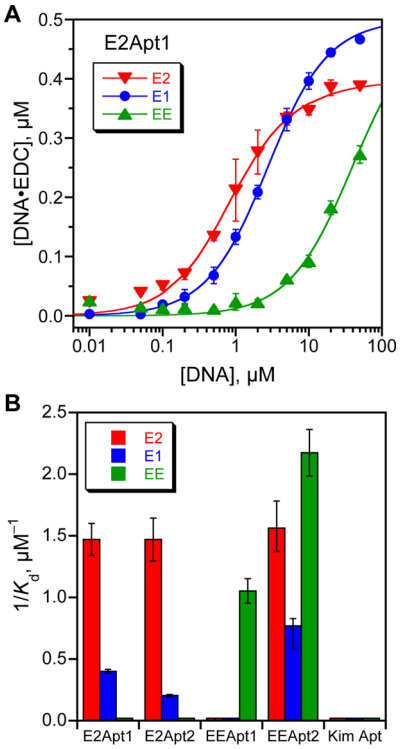

Figure 2. Dissociation constants (K_d values) for aptamers with E2 and analogues. (A) Data from equilibrium filtration assays to determine K_d values, obtained at [EDC] = 0.5 μM and plotted to allow fitting to eq 3 for EE and E1 data and eq 7 for E2 data as described in the Experimental Section. These data are for E2Apt1; see Figure S3 for comprehensive data for all aptamers in this report, as well as the aptamer of Kim et al.[35] Error bars correspond to half of range from two independent measurements. For EE and E1 plots, the midpoint of the fitted curve is found at a DNA aptamer concentration of (K_d + 0.25) μM, as derived in the Experimental Section. That is, the actual K_d value is 0.25 μM lower than the apparent midpoint of the curves. We find that the Hill coefficient for binding of E2 is slightly greater than 1 (Figure S4). See Table 1 for K_d and Hill n values. (B) Comparison of dissociation constants for each aptamer with E2 and its two analogues. For ease of comparison (larger values = tighter binding), the K_d values are shown as their reciprocals, i.e., the association constants.

Characterization of E2-Selective Aptamers by Dimethyl Sulfate (DMS) Probing. DMS probing was used to identify guanosine N7 atoms in E2Apt1 and E2Apt2 whose accessibilities decrease with increasing E2/EE concentration. These locations are indicated in the representative PAGE images in Figure 4B with decreasing band intensities, which are

DOI: 10.1021/acs.est.5b02401
Environ. Sci. Technol. 2015, 49, 9905−9913

Table 1. K_d and Hill Coefficient Values for Aptamers Studied in This Report

	K_d value, μM[a] by equilibrium filtration assay						K_d value, μM[a] by DMS probing in probing buffer[b]	
	in binding buffer			in natural water diluted 2:1 with binding buffer				
aptamer	E2	EE	E1	E2	EE	E1	E2	EE
E2Apt1	0.60 ± 0.07 (1.3 ± 0.1)	≥50	2.5 ± 0.1	0.52 ± 0.09 (1.4 ± 0.1)	≥50	2.3 ± 0.1	0.17–0.47[c]	–[d]
E2Apt2	0.56 ± 0.10 (1.5 ± 0.1)	≥50	4.9 ± 0.2	0.44 ± 0.09 (1.5 ± 0.1)	≥50	3.8 ± 0.2	0.52–0.80[c]	–[d]
EEApt1	≥50	0.95 ± 0.09	≥50	≥50	0.79 ± 0.10	≥50	—[d]	1.3 to 4.0[c]
EEApt2	0.56 ± 0.10 (1.3 ± 0.1)	0.46 ± 0.04	1.3 ± 0.1	0.87 ± 0.20 (1.3 ± 0.1)	0.50 ± 0.09	1.9 ± 0.2	–[d]	–[d]
Kim et al.[35]	≥50	≥50	≥50	nd	nd	nd	nd	nd

[a]Tabulated values represent the curve fit parameter (K_d) from data such as that in Figure 2A, Figure S3, and Figure S4. Values in parentheses represent the Hill coefficients n, for which the value is 1 when not explicitly stated. Errors correspond to curve-fit parameter errors or values calculated using covariance matrices as described in the SI. nd = not determined. $K_{1/2}$ values are derived from table values, i.e., $K_{1/2} = K_d^{1/n}$; ratios of $K_{1/2}$ values are used to compute selectivities of aptamers. [b]See SI for description of the DMS probing buffer and experiment. [c]Tabulated values represent the range of the best-fit K_d values from individual guanosine nucleotides, from data such as that shown in Figure 4C. See Table S1 for individual nucleotide K_d values. [d]K_d value could not be determined by this method because no guanosine nucleotide of EEApt2 showed dependence of DMS probing intensity on EE concentration.

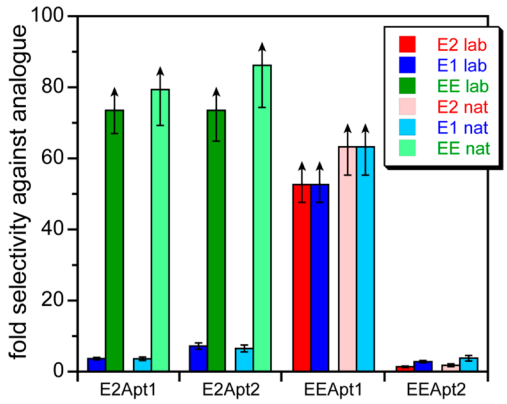

Figure 3. Aptamer selectivities, using $K_{1/2}$ values derived from Table 1, where $K_{1/2} = K_d^{1/n}$ (n = Hill coefficient). Note that when $n = 1$, $K_{1/2} = K_d$. For each E2 aptamer, the selectivity against the analogue was quantified as $K_{1/2}$(analogue)/$K_{1/2}$(E2). For each EE aptamer, the selectivity against the analogue was quantified as $K_{1/2}$(analogue)/$K_{1/2}$(EE). Data are shown for each indicated aptamer, labeled with the analogue identity as well as the water source ("lab" = laboratory water; "nat" = natural lake water). Error bars are propagated from the tabulated data by sum in quadrature for fractional error in the quotient. Data values shown with upward-pointing arrows are lower limits, because the K_d(analogue) value is a lower limit. In such cases, the error bar is simply derived from the fractional error in the denominator.

quantified and plotted in Figure 4C. For both E2Apt1 and E2Apt2, numerous guanosines showed E2-dependent changes in guanosine methylation (7 guanosines for E2Apt1; 10 for E2Apt2). E2 induced changes in nucleobase accessibilities at a much lower concentration than did EE for these E2 aptamers, in accord with the equilibrium filtration assay data. The quantitative K_d values for E2 as determined by DMS probing are in the same range as the K_d values as determined by equilibrium filtration, using the Hill coefficient model. K_d values for all nucleotide positions as determined by DMS probing are collected in Table S1.

The nucleotide sites of DMS methylation were mapped consistently to aptamer sequence components that are predicted by the mfold secondary structure prediction algorithm.[43] These sites are located within single-stranded regions rather than double-stranded regions, as illustrated in Figure 4D for E2Apt1 (see Figure S6 for analogous data for the other three aptamers). The N7 atoms of guanosine nucleotides in these relatively flexible single-stranded regions are more likely to become buried upon aptamer folding and ligand binding. Single-stranded regions can adopt more complex binding sites with greater potential for molecular recognition.

Identification of EE-Selective Aptamers. Via the same selection approach, we sought EE-selective aptamers. Because the E2 selections gave aptamers with K_d values ≤1 μM, we used 20 μM rather than 200 μM EE in the elution step, with the intention of fostering tighter EE binding. Using a constant 1 h elution time, binding was first observed as 10% at round 6, reaching 30% at round 10 (Figure S1). Individual EE aptamers were cloned, and three unique clones that did not share any common binding motifs were identified. Two unique aptamers, EEApt1 and EEApt2 (Figure S2), were studied further based on their high affinities.

Characterization of EE-Selective Aptamers by Equilibrium Filtration and DMS Probing. The same equilibrium filtration assay was used to characterize binding of EEApt1 and EEApt2 to each of EE, E2, and E1. EEApt1 and EEApt2 were found to have K_d values for EE of 0.95 and 0.46 μM, respectively (Table 1). Aptamer sensitivities of the EE aptamers are compared in Figure 2B, obtained by plotting inverse K_d values of EEApt1 and EEApt2 for each of E2, E1, and EE. EEApt1 shows the greatest affinity toward EE and significantly lower affinity toward E1 and E2. Conversely, EEApt2 binds with similar affinity to E2, EE, and E1.

Selectivity of the EE aptamers against E2 and E1 is compared in Figure 3. EEApt1 was the more selective of the two aptamers, with ≥53-fold selectivity for EE over both E1 and E2. Thus, EEApt1 had selectivity for its EE target that is comparable in magnitude to the E2 (versus EE) selectivity of both E2Apt1 and E2Apt2. In contrast, EEApt2 was only 3-fold selective for EE over E1 and essentially unselective between EE and E2. Given the relatively strong binding (low K_d value) of EEApt2, it can reasonably be considered as a general E2/EE/E1-binding aptamer (binding to EDCs other than these three was not evaluated).

DMS probing of EEApt1 revealed four guanosine sites where methylation depended upon the EE concentration, and these sites mapped onto the more flexible loop regions in the mfold-predicted secondary structure (Figure S6). This is similar to the mapping of binding-affected guanosine sites in E2Apt1 and E2Apt2. However, analogous probing experiments with EEApt2

DOI: 10.1021/acs.est.5b02401
Environ. Sci. Technol. 2015, 49, 9905–9913

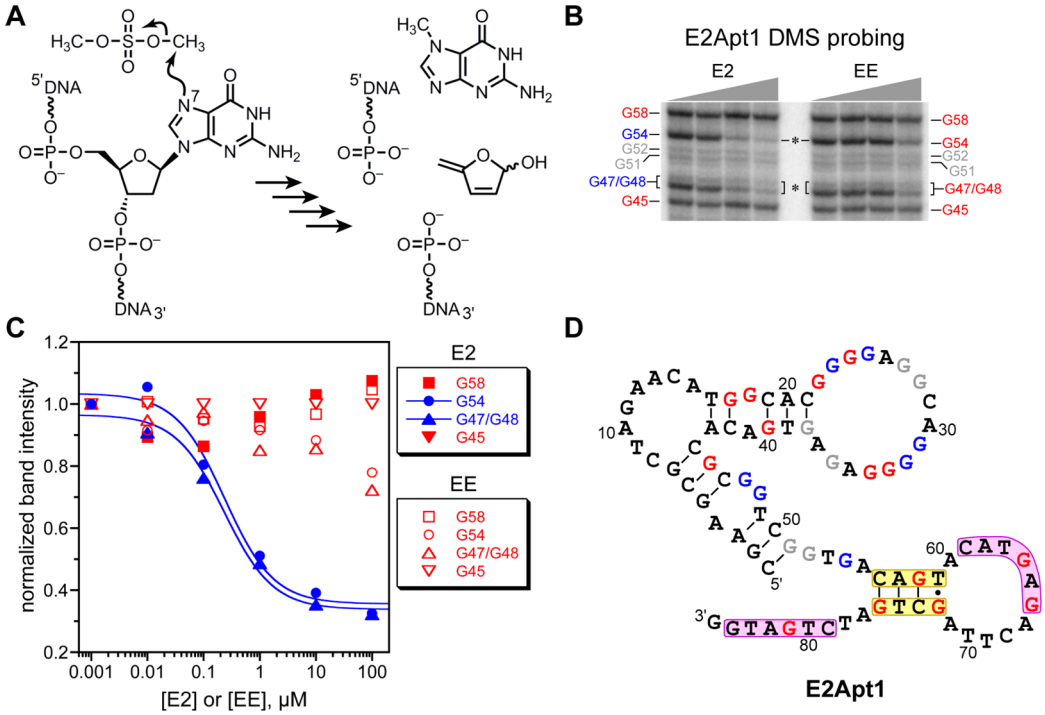

Figure 4. Dimethyl sulfate (DMS) probing. (A) Outcome of DMS methylation of guanosine N7, depurination, and strand scission. (B) Representative PAGE image for DMS probing of E2Apt1. Each band intensity correlates directly with the extent of methylation of the corresponding guanosine nucleotide. Lanes are shown for 0, 0.01, 1, and 100 μM E2/EE; see full image in Figure S5. Asterisks denote the two nucleotide positions visible on this image, G47/G48 and G54, for which E2 and EE led to substantially different concentration dependence profiles. (C) Quantification of data from the panel B experiment. Representative data for DMS probing in the presence of E2 and EE are shown with filled and open symbols, respectively. Blue and red correspond to colors used in panel D for individual guanosines. Data were fit using eq 6 as described in the Experimental Section. K_d values are in Table 1 and Table S1. (D) The lowest-energy mfold-predicted secondary structure of E2Apt1. Guanosines with substantial change in DMS accessibility as a function of E2 concentration are blue; guanosines with little or no change in accessibility are red; guanosines for which the band intensity was too low to provide useful E2 concentration dependence are gray; all nonguanosine nucleotides (and also several guanosines at the 5′- and 3′-ends for which accessibility information was not obtained) are black. In the next-lowest-energy structure (0.9 kcal/mol higher in free energy), the yellow-highlighted stem is broken, and the purple-highlighted nucleotides form a stem with one G-G mismatch. See Table S1 and Figure S6 for K_d values and secondary structures for E2Apt2, EEApt1, and EEApt2.

revealed no guanosines whose accessibilities changed substantially with EE concentration. Although the underlying reason is unclear, it is interesting that only the more general aptamer (i.e., the one with little selectivity for one EDC over another) showed no change in guanosine methylation with ligand concentration.

Sensitivity and Selectivity of the New Aptamers in Natural Water Samples. Practical applications of aptamer-based sensors require that they function well under realistic conditions.[44] We evaluated all four new aptamers (E2Apt1, E2Apt2, EEApt1, and EEApt2) for their performance in a natural water sample collected from the small urban lake in Crystal Lake Park, Urbana, IL. The lake water was filtered through a 0.22 μm filter and stored at 4 °C. The lake water was characterized for anions, cations, and organics (see Table S2 for water characterization). The TOC (~NVOC) of the lake sample, which could potentially interfere with the aptamer performance, was 4.43 mg/L. This is much greater than the amount of E2/EE/E1 used in the assays (~0.14 mg/L). The natural water was mixed with binding buffer (2:1) and spiked with 0.5 μM of one of E2, EE, or E1, and equilibrium filtration assays were performed. Neither K_d values (Table 1) nor aptamer selectivities (Figure 3) were significantly altered by the presence of the natural water, relative to K_d values and selectivities in binding buffer alone, which indicates that aptamer binding is specific to EDCs rather than general for a range of organic compounds. This finding suggests that the aptamer-based sensors should be able to detect contaminants in natural water without compromising detection limits due to interference from the environmental matrix. The aptamers were also tested in tap water from Urbana, IL (Table S2), and the sensitivities and selectivities of the aptamers were conserved.

DISCUSSION

In this study, we identified four new DNA aptamers that have submicromolar dissociation constants (K_d values) for the EDCs 17β-estradiol (E2) and its artificial derivative 17α-ethynylestradiol (EE). Although Kim et al.[35] reported an E2 aptamer with K_d of 0.13 μM, in our hands and in accord with some[45,46] but not all[31] other reports, we were unable to obtain this low K_d value, instead reproducibly finding $K_d \geq 50$ μM for their published aptamer. Because the original authors did not describe their selection procedure and provided no experimental data regarding their K_d value,[35] we cannot explain this discrepancy.

Our new aptamers have one of two behaviors with regard to ligand selectivity. Those aptamers identified by in vitro selection for binding to E2 (E2Apt1 and E2Apt2) bind strongly to both E2 and estrone (E1) but not EE. In contrast, one of the aptamers identified for binding to EE (EEApt1) binds to EE and with at least 53-fold selectivity over E2 or E1. This outcome suggests that EEApt1 discriminates between E2/

DOI: 10.1021/acs.est.5b02401
Environ. Sci. Technol. 2015, 49, 9905−9913

E1 and EE via interactions that specifically involve the ethynyl functional group of EE, whereas selectivity between E2 and E1 would require a more subtle type of interaction. The data require that the ethynyl group either interferes with aptamer binding (for the E2-selective aptamers) or is part of a requisite binding interaction (for the EE-selective aptamers). Finally, EEApt2 does not discriminate among E2, E1, and EE. This result indicates that either EEApt2 does not require specific interaction with the ethynyl group or it interacts with the functional groups common to all three compounds.

Aptamers are known to be specific to their targets when identified by appropriate selection methods. For instance, the theophylline RNA aptamer binds to its target 10 000 times better than to caffeine, which differs from theophylline by a methyl group.[47] However, not all aptamers have such high selectivites. A study that identified DNA aptamers for PCBs found that the aptamers display little selectivity toward specific congeners.[48] In natural waters, EDCs are detected at varying levels that span orders of magnitude. For example, in one study the maximum EE concentration in sewage treatment plant effluent was 3.7 pM (1.1 ng/L), while the maximum E1 concentration was 300 pM (82 ng/L).[49] This 81-fold difference in concentration would require an aptamer with an even greater difference in selectivity to enable quantification.

In most cases, our DMS probing data suggest that specific guanosine nucleotides are involved in key aspects of ligand binding. From DMS probing of E2Apt1, E2Apt2, and EEApt1, we observe that these guanosine nucleotides lie either in the interior loops or at the base of stems of the lowest-energy configuration of the aptamer predicted by mfold. This is similar to another study in which an essential binding motif (which contains four guanosines) was located in the loop regions of multiple thyroxine aptamers.[50] Additionally, the E2 aptamers are G-rich sequences with the possibility of G-quadruplex formation that involve the N7 positions. E2 binding could stabilize the G-quadruplex in the aptamer−E2 complex, decreasing the availability of the N7 position for DMS methylation. However, high-resolution structural information typically obtained from X-ray or NMR studies is necessary to explore all of these possibilities. For EEApt2, the lack of change of guanosine accessibility with EE concentration may be related to the secondary structure of the aptamer (Figure S6), which is composed of mostly stems and relatively short loop regions.

The submicromolar sensitivities and the selectivities of our new DNA aptamers are fully retained in natural water from a local lake, although the selection process was performed in a well-defined and simple laboratory binding buffer. This outcome is consistent with others' reports, in which in vitro selected aptamers have been identified in laboratory buffers yet retain useful binding activities in "real" samples such as blood and urine.[32,33,51] Moreover, the E2 aptamer from ref 35 has been employed in developing an optical sensor that was used to detect E2 as low as 5 nM in wastewater treatment plant effluents without any interference from the matrix.[27]

Small-molecule aptamer K_d values ranging from 0.05 to ≥50 μM can be used to create sensors with practical detection limits and dynamic ranges that span concentrations which are much lower than the K_d values of the aptamers used on the sensor platforms.[52−54] Lower K_d values would make more sensitive sensors (Figure S7), with a dynamic range that enables the detection of EDCs at concentrations observed in natural waters. The sensitivities and selectivities of our new aptamers, especially in natural water, bode well for practical application of the new aptamers as sensor modules. Electrochemical sensor devices that use the newly identified E2 and EE aptamers are under development.

■ ASSOCIATED CONTENT

Supporting Information

Figures S1−S7 and Tables S1 and S2. The Supporting Information is available free of charge on the ACS Publications website at DOI: 10.1021/acs.est.5b02401.

■ AUTHOR INFORMATION

Corresponding Authors

*Phone: 512-232-1626. E-mail: werth@utexas.edu.
*Phone: 217-244-4489. E-mail: scott@scs.illinois.edu.

Notes

The authors declare no competing financial interest.

■ ACKNOWLEDGMENTS

This work was partially supported by grants to C.J.W. from WaterCAMPWS, a Science and Technology Center program of the National Science Foundation under Agreement No. CTS-0120978, and from King Abdullah University of Science and Technology.

■ REFERENCES

(1) Sharpe, R. M.; Skakkebaek, N. E. Are oestrogens involved in falling sperm counts and disorders of the male reproductive tract? *Lancet* **1993**, *341*, 1392−1395.

(2) Folmar, L. C.; Denslow, N. D.; Rao, V.; Chow, M.; Crain, D. A.; Enblom, J.; Marcino, J.; Guillette, L. J., Jr. Vitellogenin induction and reduced serum testosterone concentrations in feral male carp (*Cyprinus carpio*) captured near a major metropolitan sewage treatment plant. *Environ. Health Perspect.* **1996**, *104*, 1096−1101.

(3) Thayer, K. A.; Ruhlen, R. L.; Howdeshell, K. L.; Buchanan, D. L.; Cooke, P. S.; Preziosi, D.; Welshons, W. V.; Haseman, J.; vom Saal, F. S. Altered prostate growth and daily sperm production in male mice exposed prenatally to subclinical doses of 17α-ethinyl oestradiol. *Hum. Reprod.* **2001**, *16*, 988−996.

(4) Jobling, S.; Williams, R.; Johnson, A.; Taylor, A.; Gross-Sorokin, M.; Nolan, M.; Tyler, C. R.; van Aerle, R.; Santos, E.; Brighty, G. Predicted exposures to steroid estrogens in U.K. rivers correlate with widespread sexual disruption in wild fish populations. *Environ. Health Perspect.* **2006**, *114* (Suppl 1), 32−39.

(5) Kidd, K. A.; Blanchfield, P. J.; Mills, K. H.; Palace, V. P.; Evans, R. E.; Lazorchak, J. M.; Flick, R. W. Collapse of a fish population after exposure to a synthetic estrogen. *Proc. Natl. Acad. Sci. U. S. A.* **2007**, *104*, 8897−8901.

(6) Vilahur, N.; Bustamante, M.; Byun, H. M.; Fernandez, M. F.; Santa Marina, L.; Basterrechea, M.; Ballester, F.; Murcia, M.; Tardón, A.; Fernández-Somoano, A.; Estivill, X.; Olea, N.; Sunyer, J.; Baccarelli, A. A. Prenatal exposure to mixtures of xenoestrogens and repetitive element DNA methylation changes in human placenta. *Environ. Int.* **2014**, *71*, 81−87.

(7) Kolpin, D. W.; Furlong, E. T.; Meyer, M. T.; Thurman, E. M.; Zaugg, S. D.; Barber, L. B.; Buxton, H. T. Pharmaceuticals, hormones, and other organic wastewater contaminants in U.S. streams, 1999−2000: a national reconnaissance. *Environ. Sci. Technol.* **2002**, *36*, 1202−1211.

(8) Van den Belt, K.; Berckmans, P.; Vangenechten, C.; Verheyen, R.; Witters, H. Comparative study on the in vitro/in vivo estrogenic potencies of 17β-estradiol, estrone, 17α-ethynylestradiol and nonylphenol. *Aquat. Toxicol.* **2004**, *66*, 183−195.

(9) Pillon, A.; Boussioux, A. M.; Escande, A.; Ait-Aissa, S.; Gomez, E.; Fenet, H.; Ruff, M.; Moras, D.; Vignon, F.; Duchesne, M. J.; Casellas, C.; Nicolas, J. C.; Balaguer, P. Binding of estrogenic compounds to

DOI: 10.1021/acs.est.5b02401
Environ. Sci. Technol. 2015, 49, 9905−9913

recombinant estrogen receptor-α: Application to environmental analysis. *Environ. Health Perspect.* **2005**, *113*, 278−284.
(10) Hutchins, S. R.; White, M. V.; Hudson, F. M.; Fine, D. D. Analysis of lagoon samples from different concentrated animal feeding operations for estrogens and estrogen conjugates. *Environ. Sci. Technol.* **2007**, *41*, 738−744.
(11) Grover, D. P.; Zhang, Z. L.; Readman, J. W.; Zhou, J. L. A comparison of three analytical techniques for the measurement of steroidal estrogens in environmental water samples. *Talanta* **2009**, *78*, 1204−1210.
(12) Hirobe, M.; Goda, Y.; Okayasu, Y.; Tomita, J.; Takigami, H.; Ike, M.; Tanaka, H. The use of enzyme-linked immunosorbent assays (ELISA) for the determination of pollutants in environmental and industrial wastes. *Water Sci. Technol.* **2006**, *54*, 1−9.
(13) Manickum, T.; John, W. The current preference for the immuno-analytical ELISA method for quantitation of steroid hormones (endocrine disruptor compounds) in wastewater in South Africa. *Anal. Bioanal. Chem.* **2015**, *407*, 4949−4970.
(14) Sawaya, W. N.; Lone, K. P.; Husain, A.; Dashti, B.; Al-Zenki, S. Screening for estrogenic steroids in sheep and chicken by the application of enzyme-linked immunosorbent assay and a comparison with analysis by gas chromatography-mass spectrometry. *Food Chem.* **1998**, *63*, 563−569.
(15) Farré, M.; Brix, R.; Kuster, M.; Rubio, F.; Goda, Y.; López de Alda, M. J.; Barceló, D. Evaluation of commercial immunoassays for the detection of estrogens in water by comparison with high-performance liquid chromatography tandem mass spectrometry HPLC-MS/MS (QqQ). *Anal. Bioanal. Chem.* **2006**, *385*, 1001−1011.
(16) Viganò, L.; Benfenati, E.; van Cauwenberge, A.; Eidem, J. K.; Erratico, C.; Goksøyr, A.; Kloas, W.; Maggioni, S.; Mandich, A.; Urbatzka, R. Estrogenicity profile and estrogenic compounds determined in river sediments by chemical analysis, ELISA and yeast assays. *Chemosphere* **2008**, *73*, 1078−1089.
(17) Lopez de Alda, M. J.; Barcelo, D. Review of analytical methods for the determination of estrogens and progestogens in waste waters. *Fresenius' J. Anal. Chem.* **2001**, *371*, 437−447.
(18) Committee on Methods of Producing Monoclonal Antibodies of the Institute for Laboratory Animal Research of the National Research Council. Animal-Welfare Issues Related to the Ascites Method for Producing Monoclonal Antibodies. In *Monoclonal Antibody Production*; National Academy Press: Washington, DC, 1999.
(19) O'Sullivan, C. K. Aptasensors—the future of biosensing? *Anal. Bioanal. Chem.* **2002**, *372*, 44−48.
(20) Nutiu, R.; Li, Y. In vitro selection of structure-switching signaling aptamers. *Angew. Chem., Int. Ed.* **2005**, *44*, 1061−1065.
(21) Liu, J.; Lu, Y. Fast Colorimetric Sensing of Adenosine and Cocaine Based on a General Sensor Design Involving Aptamers and Nanoparticles. *Angew. Chem., Int. Ed.* **2006**, *45*, 90−94.
(22) Zayats, M.; Huang, Y.; Gill, R.; Ma, C. A.; Willner, I. Label-free and reagentless aptamer-based sensors for small molecules. *J. Am. Chem. Soc.* **2006**, *128*, 13666−13667.
(23) Baker, B. R.; Lai, R. Y.; Wood, M. S.; Doctor, E. H.; Heeger, A. J.; Plaxco, K. W. An electronic, aptamer-based small-molecule sensor for the rapid, label-free detection of cocaine in adulterated samples and biological fluids. *J. Am. Chem. Soc.* **2006**, *128*, 3138−3139.
(24) Willner, I.; Zayats, M. Electronic aptamer-based sensors. *Angew. Chem., Int. Ed.* **2007**, *46*, 6408−6418.
(25) Song, S.; Wang, L.; Li, J.; Zhao, J.; Fan, C. Aptamer-based biosensors. *TrAC, Trends Anal. Chem.* **2008**, *27*, 108−117.
(26) Vikesland, P. J.; Wigginton, K. R. Nanomaterial enabled biosensors for pathogen monitoring - A review. *Environ. Sci. Technol.* **2010**, *44*, 3656−3669.
(27) Yildirim, N.; Long, F.; Gao, C.; He, M.; Shi, H. C.; Gu, A. Z. Aptamer-based optical biosensor for rapid and sensitive detection of 17β-estradiol in water samples. *Environ. Sci. Technol.* **2012**, *46*, 3288−3294.
(28) Kent, A. D.; Spiropulos, N. G.; Heemstra, J. M. General approach for engineering small-molecule-binding DNA split aptamers. *Anal. Chem.* **2013**, *85*, 9916−9923.
(29) Deng, C.; Chen, J.; Nie, Z.; Wang, M.; Chu, X.; Chen, X.; Xiao, X.; Lei, C.; Yao, S. Impedimetric aptasensor with femtomolar sensitivity based on the enlargement of surface-charged gold nanoparticles. *Anal. Chem.* **2009**, *81*, 739−745.
(30) Fan, L.; Zhao, G.; Shi, H.; Liu, M.; Wang, Y.; Ke, H. A femtomolar level and highly selective 17β-estradiol photoelectrochemical aptasensor applied in environmental water samples analysis. *Environ. Sci. Technol.* **2014**, *48*, 5754−5761.
(31) Ke, H.; Liu, M.; Zhuang, L.; Li, Z.; Fan, L.; Zhao, G. A femtomolar level 17β-estradiol electrochemical aptasensor constructed on hierarchical dendritic gold modified boron-doped diamond electrode. *Electrochim. Acta* **2014**, *137*, 146−153.
(32) Swensen, J. S.; Xiao, Y.; Ferguson, B. S.; Lubin, A. A.; Lai, R. Y.; Heeger, A. J.; Plaxco, K. W.; Soh, H. T. Continuous, real-time monitoring of cocaine in undiluted blood serum via a microfluidic, electrochemical aptamer-based sensor. *J. Am. Chem. Soc.* **2009**, *131*, 4262−4266.
(33) Ferguson, B. S.; Hoggarth, D. A.; Maliniak, D.; Ploense, K.; White, R. J.; Woodward, N.; Hsieh, K.; Bonham, A. J.; Eisenstein, M.; Kippin, T. E.; Plaxco, K. W.; Soh, H. T. Real-time, aptamer-based tracking of circulating therapeutic agents in living animals. *Sci. Transl. Med.* **2013**, *5*, 213ra165.
(34) An, J. H.; Park, S. J.; Kwon, O. S.; Bae, J.; Jang, J. High-performance flexible graphene aptasensor for mercury detection in mussels. *ACS Nano* **2013**, *7*, 10563−10571.
(35) Kim, Y. S.; Jung, H. S.; Matsuura, T.; Lee, H. Y.; Kawai, T.; Gu, M. B. Electrochemical detection of 17β-estradiol using DNA aptamer immobilized gold electrode chip. *Biosens. Bioelectron.* **2007**, *22*, 2525−2531.
(36) Long, F.; Shi, H.; Wang, H. Fluorescence resonance energy transfer based aptasensor for the sensitive and selective detection of 17β-estradiol using a quantum dot-bioconjugate as a nano-bioprobe. *RSC Adv.* **2014**, *4*, 2935−2941.
(37) Liu, J.; Bai, W.; Niu, S.; Zhu, C.; Yang, S.; Chen, A. Highly sensitive colorimetric detection of 17β-estradiol using split DNA aptamers immobilized on unmodified gold nanoparticles. *Sci. Rep.* **2014**, *4*, 7571.
(38) Lin, Z.; Chen, L.; Zhang, G.; Liu, Q.; Qiu, B.; Cai, Z.; Chen, G. Label-free aptamer-based electrochemical impedance biosensor for 17β-estradiol. *Analyst* **2012**, *137*, 819−822.
(39) Tuerk, C.; Gold, L. Systematic evolution of ligands by exponential enrichment: RNA ligands to bacteriophage T4 DNA polymerase. *Science* **1990**, *249*, 505−510.
(40) Ellington, A. D.; Szostak, J. W. In vitro selection of RNA molecules that bind specific ligands. *Nature* **1990**, *346*, 818−822.
(41) Levy, M.; Ellington, A. D. ATP-dependent allosteric DNA enzymes. *Chem. Biol.* **2002**, *9*, 417−426.
(42) Maxam, A. M.; Gilbert, W. A new method for sequencing DNA. *Proc. Natl. Acad. Sci. U. S. A.* **1977**, *74*, 560−564.
(43) Zuker, M. Mfold web server for nucleic acid folding and hybridization prediction. *Nucleic Acids Res.* **2003**, *31*, 3406−3415.
(44) Li, Y.; Lu, Y., Eds. *Functional Nucleic Acids for Analytical Applications*; Springer Science + Business Media, LLC: New York, 2009.
(45) Huy, G. D.; Jin, N.; Yin, B. C.; Ye, B. C. A novel separation and enrichment method of 17β-estradiol using aptamer-anchored microbeads. *Bioprocess Biosyst. Eng.* **2011**, *34*, 189−195.
(46) Langan, T. J.; Nyakubaya, V. T.; Casto, L. D.; Dolan, T. D.; Archer-Hartmann, S. A.; Yedlapalli, S. L.; Sooter, L. J.; Holland, L. A. Assessment of aptamer-steroid binding using stacking-enhanced capillary electrophoresis. *Electrophoresis* **2012**, *33*, 866−869.
(47) Jenison, R. D.; Gill, S. C.; Pardi, A.; Polisky, B. High-resolution molecular discrimination by RNA. *Science* **1994**, *263*, 1425−1429.
(48) Mehta, J.; Rouah-Martin, E.; Van Dorst, B.; Maes, B.; Herrebout, W.; Scippo, M. L.; Dardenne, F.; Blust, R.; Robbens, J. Selection and characterization of PCB-binding DNA aptamers. *Anal. Chem.* **2012**, *84*, 1669−1676.
(49) Baronti, C.; Curini, R.; D'Ascenzo, G.; Di Corcia, A.; Gentili, A.; Samperi, R. Monitoring Natural and Synthetic Estrogens at Activated

DOI: 10.1021/acs.est.5b02401
Environ. Sci. Technol. 2015, 49, 9905−9913

Sludge Sewage Treatment Plants and in a Receiving River Water. *Environ. Sci. Technol.* **2000**, *34*, 5059−5066.
(50) Lévesque, D.; Beaudoin, J. D.; Roy, S.; Perreault, J. P. In vitro selection and characterization of RNA aptamers binding thyroxine hormone. *Biochem. J.* **2007**, *403*, 129−138.
(51) Roncancio, D.; Yu, H.; Xu, X.; Wu, S.; Liu, R.; Debord, J.; Lou, X.; Xiao, Y. A label-free aptamer-fluorophore assembly for rapid and specific detection of cocaine in biofluids. *Anal. Chem.* **2014**, *86*, 11100−11106.
(52) Wu, J.; Chu, H.; Mei, Z.; Deng, Y.; Xue, F.; Zheng, L.; Chen, W. Ultrasensitive one-step rapid detection of ochratoxin A by the folding-based electrochemical aptasensor. *Anal. Chim. Acta* **2012**, *753*, 27−31.
(53) Jiang, B.; Wang, M.; Chen, Y.; Xie, J.; Xiang, Y. Highly sensitive electrochemical detection of cocaine on graphene/AuNP modified electrode via catalytic redox-recycling amplification. *Biosens. Bioelectron.* **2012**, *32*, 305−308.
(54) Xue, F.; Wu, J.; Chu, H.; Mei, Z.; Ye, Y.; Liu, J.; Zhang, R.; Peng, C.; Zheng, L.; Chen, W. Electrochemical aptasensor for the determination of bisphenol A in drinking water. *Microchim. Acta* **2013**, *180*, 109−115.

DOI: 10.1021/acs.est.5b02401
Environ. Sci. Technol. 2015, 49, 9905−9913